# Photoluminescent Diamond Nanoparticles for Cell Labeling: Study of the Uptake Mechanism in Mammalian Cells

**Orestis Faklaris,[†] Vandana Joshi,[‡] Theano Irinopoulou,[§] Patrick Tauc,[∥] Mohamed Sennour,[⊥] Hugues Girard,[¶] Céline Gesset,[¶] Jean-Charles Arnault,[¶] Alain Thorel,[⊥] Jean-Paul Boudou,[‡] Patrick A. Curmi,[‡,*] and François Treussart[†,*]**

[†]Laboratoire de Photonique Quantique et Moléculaire, Ecole Normale Supérieure de Cachan and CNRS UMR 8537, Cachan, France, [‡]Institut National de la Santé et de la Recherche Médicale (INSERM), UMR829; Université Evry-Val d'Essonne; Laboratoire Structure-Activité des Biomolécules Normales et Pathologiques, Evry, France, [§]Institut du Fer à Moulin, Université Pierre et Marie Curie and INSERM, UMR-S 839, Paris, France, [∥]Laboratoire de Biologie et de Pharmacologie Appliquée, Ecole Normale Supérieure de Cachan and CNRS UMR 8113, Cachan, France, [⊥]Laboratoire Pierre-Marie Fourt, Centre des Matériaux de l'Ecole des Mines de Paris and CNRS UMR 7633, Evry, France, and [¶]Diamond Sensor Laboratory, CEA-LIST, Gif-sur-Yvette, France

**ABSTRACT** Diamond nanoparticles (nanodiamonds) have been recently proposed as new labels for cellular imaging. For small nanodiamonds (size <40 nm), resonant laser scattering and Raman scattering cross sections are too small to allow single nanoparticle observation. Nanodiamonds can, however, be rendered photoluminescent with a perfect photostability at room temperature. Such a remarkable property allows easier single-particle tracking over long time scales. In this work, we use photoluminescent nanodiamonds of size <50 nm for intracellular labeling and investigate the mechanism of their uptake by living cells. By blocking selectively different uptake processes, we show that nanodiamonds enter cells mainly by endocytosis, and converging data indicate that it is clathrin-mediated. We also examine nanodiamond intracellular localization in endocytic vesicles using immunofluorescence and transmission electron microscopy. We find a high degree of colocalization between vesicles and the biggest nanoparticles or aggregates, while the smallest particles appear free in the cytosol. Our results pave the way for the use of photoluminescent nanodiamonds in targeted intracellular labeling or biomolecule delivery.

**KEYWORDS:** diamond · nanoparticles · photoluminescence · biolabel · endocytosis

Solid-state nanoparticles hold great promises for biomedical applications, notably thanks to the possibility to combine biological and inorganic materials with the prospect to develop innovative diagnostic and therapeutic tools. Among them, nanoparticles such as quantum dots,[1,2] gold nanobeads,[3] or silicon beads[4] are used to label a biomolecule with high specificity, to track their fate in cultured cells and in organisms, or even to deliver bioactive molecules or drugs. Organic dyes and fluorophores are nowadays the most widely used fluorescent labels of biomolecules. However, they photobleach rapidly under continuous illumination,[5] which makes their quantification and long-term follow-up difficult. Interestingly, semiconductor nanocrystals, or quantum dots (QDs), have a better stability and a lower photobleaching yield than organic dyes. They also offer the possibility of multicolor staining by size tuning.[2] On the other hand, such nanoparticles present major drawbacks, such as a potential cytotoxicity on long-term scale due to the chemical composition of their core[6] or the intermittency of their photoluminescence (photoblinking), which makes an efficient tracking of individual nanoparticles difficult.[7]

Compared to these nanoparticles, photoluminescent nanodiamonds (PNDs) appear as promising alternative biomarkers. Their photoluminescence, with emission in the red and near-infrared spectral region (575−750 nm), results from nitrogen-vacancy (NV) color centers embedded in the diamond matrix.[8] These emitters present a perfect photostability with no photobleaching or photoblinking, and a photoluminescence intensity at saturation which is only three times smaller than that of a single commercial QD (under the same laser excitation at 532 nm) a situation which can be reversed in favor of NDs by the use of particles containing a large number of color centers.[9] Such remarkable photoluminescent properties have made possible long-term single-particle tracking in living cells.[9−11]

Moreover, thanks to a large specific surface area, the nanodiamond can be used as a platform to graft a large variety of

See the accompanying Perspective by Ho on p 3825.

*Address correspondence to francois.treussart@ens-cachan.fr, pcurmi@univ-evry.fr.

Received for review August 14, 2009 and accepted October 18, 2009.

**Published online October 28, 2009.**
10.1021/nn901014j CCC: $40.75

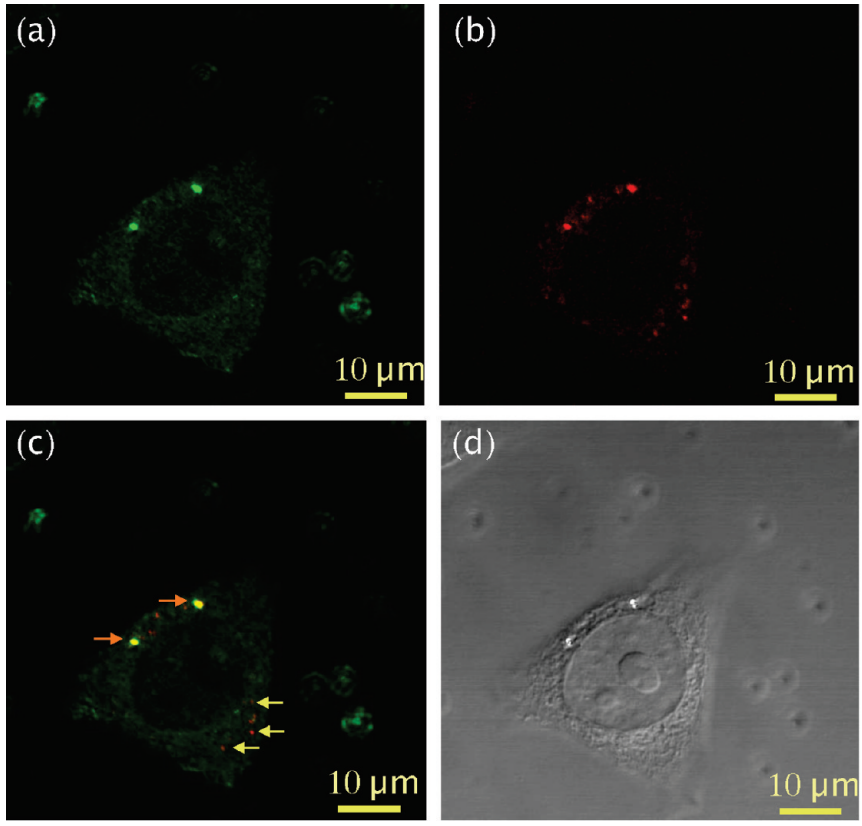


**Figure 1. Imaging of photoluminescent nanodiamonds internalized in HeLa cells in three different contrast modes of a Leica TCS SP2 microscope: (a) raster scan of backscattered excitation laser light (wavelength 488 nm); (b) photoluminescence confocal raster scan in the NV color center emission spectrum region (red channel, refer to Materials and Methods); (c) overlay of (a) and (b), orange arrows, pointing to the right, exhibit nanoparticles that are observed in both backscattered and fluorescence modes, while the yellow arrows pointing to the left show some nanodiamonds that are detected only in the photoluminescence mode; (d) DIC image obtained in transmission with white light illumination. The confocal section (b) was acquired with laser focusing into the plane located 2.5 μm above the coverglass surface on which the cell was grown (image #5 of the cross section series of Figure S4b in the Supporting Information).**

bioactive moieties[12−15] with the perspective to use these particles, for instance, as intracellular compartment labels[16] or as long-term traceable delivery vehicles for biomolecule translocation in the cell.[14−18] Considering the recent demonstrations of PND mass production[11,19] and the numerous experiments showing their low cytotoxicity,[17,20−22] one can envision large-scale applications of these biolabels. However, such outstanding prospects require a better understanding of the mechanism underlying their cellular uptake.

To that end, we study in the present work the cellular fate of photoluminescent nanodiamonds of size <50 nm. We first show that, for such a small size nanodiamond, excitation laser scattering yields no signal and that only photoluminescence allows their detection with a sufficiently high signal-to-background ratio. We then carry out a systematic investigation of the cellular uptake and pathway of PNDs in human cancer cells (HeLa cells) and observe that the internalization of PNDs stems mainly from endocytosis. The localization of PNDs in cells is studied using simultaneous detection of PNDs and immunofluorescence methods to label the endosomes and the lysosomes.

## RESULTS AND DISCUSSION

**Nanodiamond Observation at the Single Particle Level in Cells.** In the present work, we use nanodiamonds produced by milling of 150−200 μm diamond microcrystals after the activation of their photoluminescence by the creation of NV color centers in the diamond matrix (see Materials and Methods). We selected by differential centrifugations of an aqueous suspension of the milled product a subset of nanodiamonds having a mean hydrodynamic diameter centered on 46 nm. Since the diamond refractive index value of 2.4 is about two times larger than that of the cellular medium, diamond can yield a higher backscattered intensity of the excitation laser light than the cell compartments. Such a scattering signal can then be used to image nanodiamonds in the cell with a good contrast.[10,23] However, the scattering intensity decreases rapidly with the particle size, due to its sixth order dependence on the particle diameter (Rayleigh scattering). It was shown that the smallest nanodiamonds detectable by this technique have sizes of 37 nm.[24]

Accordingly, we observe that ND's size is too small to image the particles in the cell by backscattered light with a reasonably high signal-to-background ratio, which can compete with that of the photoluminescence signal. Figure 1 shows a HeLa cell imaged with a standard confocal microscope (Leica TCS SP2) in three different contrast modes: (a) backscattering (sometimes referred as the "reflection" mode) of the incident laser operating in cw regime at an excitation wavelength of 488 nm, (b) photoluminescence excited by the same laser and detected in the NV color center spectral region, and (d) DIC (differential interference contrast) obtained in transmission under white light illumination of the sample. Two PNDs are detected by the different contrast modes and probably correspond to particles bigger than 50 nm (orange arrows pointing to the right on Figure 1c). On the contrary, a few PNDs are only detected in the fluorescence mode (three of them are marked with yellow arrows pointing to the left on Figure 1c). Complementary observations done with a homemade confocal microscope characterized by single color center sensitivity (Figure S1

of the Supporting Information) confirm this result (Figure S2). These experiments indicate that fluorescence microscopy is the most appropriate method to detect the smallest PNDs internalized by cells. Moreover, a higher PND photoluminescence intensity can be achieved by increasing the number of color centers created per particle. A recent report on PNDs which were produced by a technique similar to the one used here shows that, by optimizing the NV color center creation, one can reach a concentration up to 12 NV centers in nanodiamonds of size around 10 nm.[19] Such a result is very promising for the tracking of very small PNDs in the cell.

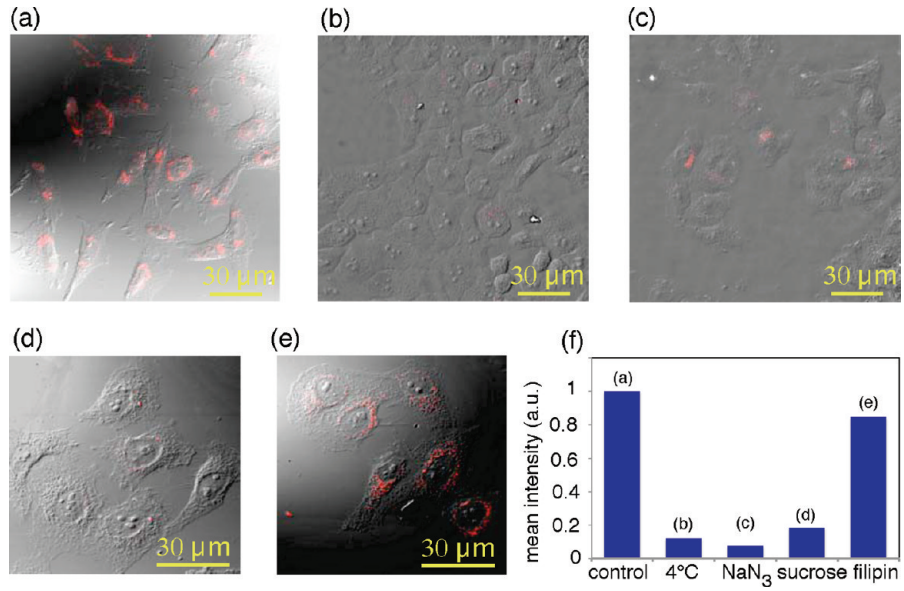


**Figure 2. Nanodiamonds are uptaken by HeLa cells through endocytosis. Merged photoluminescence confocal raster scans (red channel) and DIC images of PNDs (concentration 20 μg/mL) incubated for 2 h with cells (a) at 37 °C (control) and (b) at 4 °C, or at 37 °C but after pretreatment with either (c) $NaN_3$ (10 mM) or (d) sucrose (0.45 M) or (e) filipin (5 μg/ml). Confocal scans are acquired at $z = 1.5$ μm above the coverglass surface, laser excitation power = 0.5 mW. (f) Mean photoluminescence intensity per cell (in the red channel) for the different cell treatments, normalized to that of control cells and evaluated as described in Materials and Methods.**

**Mechanism of PND Uptake by Cells.** It is well-established that NDs can spontaneously enter cultured cells, as demonstrated by confocal microscopy[14,20,21] (Figure S4 in the Supporting Information). In this work, we further investigated the internalization mechanism of PNDs in HeLa cells.

We quantified the dynamics of the PND's uptake by cells by monitoring the overall cell fluorescence intensity (refer to Materials and Methods), and we found that the uptake follows an exponential behavior with time, with a characteristic uptake half-life of 2.6 h (Figure S3). This measurement is compatible with the 3 h uptake half-life observed for 70 nm PNDs[25] and the 1.9 h reported for 50 nm gold nanoparticles.[26]

Endocytosis is considered as the dominant uptake mechanism of extracellular materials of size up to about 150 nm.[27,28] We therefore evaluated the contribution of endocytosis to ND internalization by HeLa cells. For this purpose, the cells were incubated with PNDs (concentration 20 μg/mL) under different conditions: (i) at 37 °C (control), (ii) at 4 °C, and (iii) after pretreatment with $NaN_3$. The latter treatment disturbs the production of ATP and blocks the endocytosis,[29] which is an energy-dependent process. Incubation of the cells at 4 °C is also known to block endocytosis.

For the analysis of ND's uptake under different cellular treatments, we used the Leica TCS SP2 confocal microscope. Figure 2 shows that, when endocytosis is hindered by low temperature or $NaN_3$, the photoluminescence signal from PNDs strongly decreases (Figure 2b,c) compared to the control (Figure 2a). Similar results were obtained using the home-built confocal microscope, which is able to detect all PNDs, including those containing only a single color center, presumably the smallest nanoparticles (Figure S5 in the Supporting Information). These observations, together with the fact that the majority of the NDs from the sample exhibit some photoluminescence (Figure 5), strongly suggest that very few NDs are internalized when endocytosis is blocked.

To further document the endocytosis mechanisms involved in the cellular uptake of nanodiamonds, we investigated the receptor-mediated endocytosis (RME) pathway. In RME, a ligand first binds to a cell surface receptor and is then internalized through an invagination of the plasma membrane. Among the different RME processes, the clathrin-mediated pathway is the most frequent one. Clathrin is a protein which coats cell membrane invaginations leading to the budding of clathrin-coated vesicles.[30,31] Other main RME processes, which are clathrin-independent, occur through the caveolae pathway. Caveolae are invaginations rich in cholesterol.[32] In our experiments, cells were incubated with PNDs under conditions that inhibit either the clathrin or the caveolae pathway. Interestingly, we observe that pretreatment of cells with sucrose, a hypertonic treatment known to disrupt the formation of clathrin-coated vesicles,[33,34] reduces to a high degree the PND uptake (Figure 2d). To block the caveolae pathway, cells were pretreated with filipin, which disrupts the formation of the cholesterol domains.[34,35] In contrast to the clathrin pathway blocking experiment, we observe that pretreatment with filipin does not hinder the internalization of PNDs (Figure 2e). These results indicate that PNDs are mainly internalized by cells by the clathrin-mediated pathway.

For a more quantitative analysis, we evaluated the mean photoluminescence intensity per cell (in the red channel, corresponding to NV color center emission), in a way similar to the one used for the dynamic measurement of PND cellular internalization. Figure 2f shows the change of the mean photoluminescence intensity per cell, normalized to that of control cells. This graph summarizes quantitatively the effects of the different cell treatments and supports the conclusion that the uptake mechanism of PNDs is endocytosis, with strong indications that it is clathrin-mediated. The latter statement is reinforced by a complementary analysis done on nanodiamond surface functions. We studied by FTIR spectroscopy the modifications of ND surface function signatures before and after their mixture with serum-supplemented culture medium (refer to Supporting Information Figure S9). We observed that proteins of the serum are adsorbed onto the nanodiamond surface, which may facilitate a receptor-mediated endocytosis. Concomitantly, we noticed that the addition of serum greatly improves the stability of the nanodiamond suspension in the culture medium, which is also related to surface modifications impacting its electric charge.

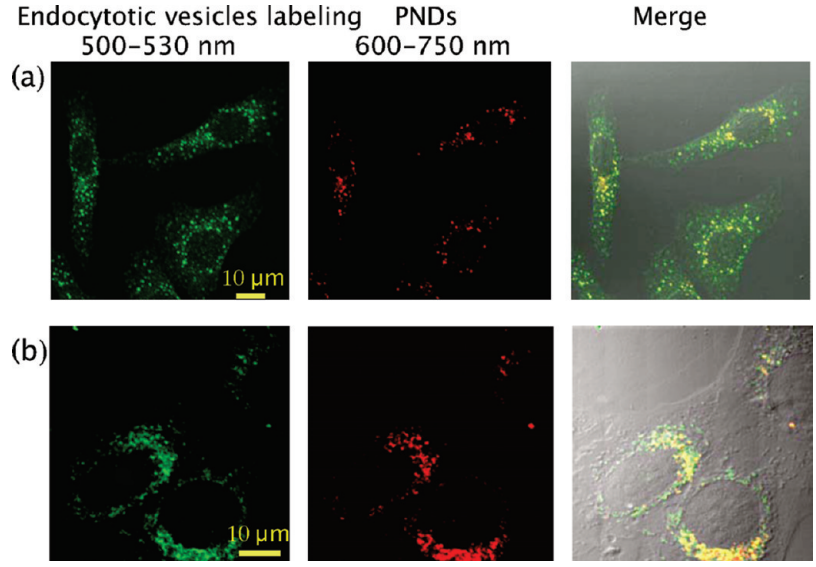


**Figure 3. Localization of 46 nm photoluminescent nanodiamonds in HeLa cells. Confocal fluorescence raster scan (Leica TCS SP2 microscope) of HeLa cell incubated with PNDs (10 μg/ml) in normal (control) conditions, then fixed. Endosomes or lysosomes are labeled with dyes. From left to right: raster scan in the green channel (500−530 nm) showing the endocytic compartments and in the red channel (600−750 nm) showing the PNDs. Images on the right represent the merged the green and red scans. (a) Colocalization study of PNDs with early endosomes labeled with EEA1-FITC fluorescent conjugate. (b) Colocalization of PNDs with lysosomes labeled with LysoTracker green dye. PNDs colocalized with endosomes or lysosomes appear in yellow in the merged fluorescence scans.**

The present results on the nanodiamond internalization pathway are close to those obtained on the same HeLa cell line for other types of nanoparticles with similar sizes, like gold nanoparticles[26] or single-walled carbon nanotubes noncovalently conjugated with DNA molecules or proteins.[36]

**Intracellular Localization of PNDs.** After an endocytic uptake, the internalized compound is expected to be found in intracellular endosomal and lysosomal vesicles, before eventually being released in the cytosol or expelled from the cell. Endosomes are vesicles involved in the transport of extracellular materials in the cell cytoplasm. After internalization, endosomes are either recycled to the plasma membrane and the receptors can be used for a novel cycle or fused with lysosomes.[30]

In a previous study, we concluded from immunofluorescence analyses that 25 nm PNDs are partially colocalized with early endosomes.[21] Here we provide similar but more complete results obtained with PNDs produced in a different way. Apart from a difference in the mean size between the two kinds of PNDs, the nanoparticles do not have the same morphologies, as it can be seen in TEM images (Figure 5c and also ref 19): the shape of the 46 nm nanoparticles produced by milling is more spherical, while the 25 nm commercial NDs present sharper edges.[37] These differences may impact the uptake efficiency and justify a new localization study.

Early endosomes and lysosomes were marked with fluorescent labels emitting in the green spectral region (500−550 nm), with no overlap with the red and near-infrared emission of NV color centers (Figure 5d). Scanning confocal imaging was carried out with the Leica TCS SP2 microscope. The red channel detection spectral range selected for PNDs imaging is 600−750 nm to avoid again any overlap with the emission of the cellular components labels (see Figure S6 in the Supporting Information for a control experiment). Figure 3 shows a high degree of colocalization of PNDs with both early endosomes and lysosomes, which supports the fact that NDs follow the course of the endocytic cycle. This endosomal localization of PNDs again agrees with reports on other kind of similar size nanoparticles, such as QDs[38] or gold nanobeads.[26,39]

To further elucidate the fate of the smallest and less bright PNDs that cannot be detected with the Leica TCS SP2 microscope, we examined the same samples with two complementary techniques: with the home-built confocal setup (Figure S1) detecting the smallest photoluminescent PNDs and with electron mi-

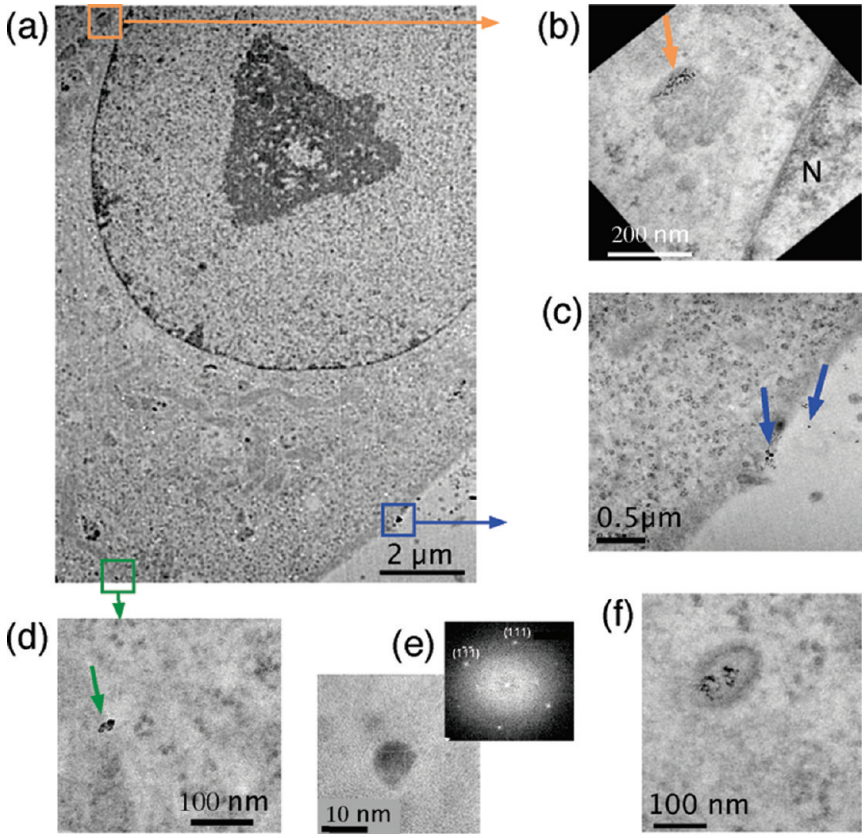


**Figure 4. Transmission electron microscopy images of a HeLa cell incubated with PNDs for 2 h. (a) Large-scale image. (b) PNDs trapped in intracellular vesicles; N indicates the position of cell nucleus. (c) PNDs outside the cell and on the cell membrane (blue arrows), probably during the early stage of the internalization process because the half-life uptake (2.6 h) is longer than the incubation time. (d) Free PNDs in the cytoplasm. (e) Zoomed-in image of one 10 nm PND. Inset: local area Fourier transform diffractogram of this PND. (f) PNDs trapped in an intracellular vesicle of another cell from the same sample.**

croscopy. Observations with the home-built confocal microscope show a partial colocalization (Figure S7), which is also confirmed by transmission electron microscopy (TEM) imaging. In the latter technique, ND particles appear as dark spots on the gray cytoplasmic background.[40]

In the large-scale TEM image (Figure 4a) of a part of a HeLa cell incubated with PNDs, one can observe the nanoparticles in the cytoplasm. They are either trapped in vesicles (Figure 4b,f) or free in the cytosol (Figure 4d and Figure S8b). NDs trapped in vesicles form aggregates (Figure 4b,f and Figure S8a) and represent the majority of the nanodiamonds observed by TEM inside the cell cytoplasm. This is in agreement with our colocalization studies and with the confined motion of PNDs observed with wide-field microscopy.[11,21] Nanodiamonds which are free in the cytosol correspond to the smallest particles that can be observed at their primary size (<5−10 nm) or as small aggregates of a few particles. These free nanoparticles either have been released from the endosomes or may have been directly internalized *via* passive transport (like facilitated diffusion) through the cell membrane. Interestingly, all internalized nanodiamonds, even of the smallest size (<5 nm), are observed in perinuclear regions and none of them seems to be present inside the nucleus. A necessary requirement to use PNDs as biomolecule markers is their low cytotoxicity. As cytotoxicity depends on the cellular type used and the size, shape, and charge of the nanoparticles,[42] we performed cytotoxicity tests for the PNDs used here. We show that they are not toxic *in vitro* after 24 h of incubation with cells (Figure S10).

## CONCLUSION

In this work, we used 46 nm mean size photoluminescent diamond nanoparticles produced by micrometer-size diamond milling as cell labels. We showed that photoluminescence detection allows imaging of the smallest nanodiamonds that cannot be observed by the backscattered light of the excitation laser. This result underlines the superiority of photoluminescence for tiny nanodiamonds imaging in complex environments such as the intracellular medium. With the use of a commercial laser scanning confocal microscope, we showed that the internalization of PNDs in HeLa cells occurs through endocytosis, and we have strong indications that it is receptor-mediated *via* the clathrin pathway.

We observed that most of the nanodiamonds are localized in intracellular endocytic vesicles in the perinuclear region, except for a small portion, in particular the smallest particles, that appear to be free in the cytoplasm. The latter may be of interest for biomolecule delivery applications, owing to its high diffusion coefficient in the cytosol. However, as the cell represents an inhomogeneous medium, a detailed understanding of the distribution of nanoparticles in the cytoplasm is only the first step toward the utilization of diamond nanoparticles for biological applications (translocation and tracking of biomolecules in cell, labeling of specific compartments or tumorous cells, *etc.*). The observations re-

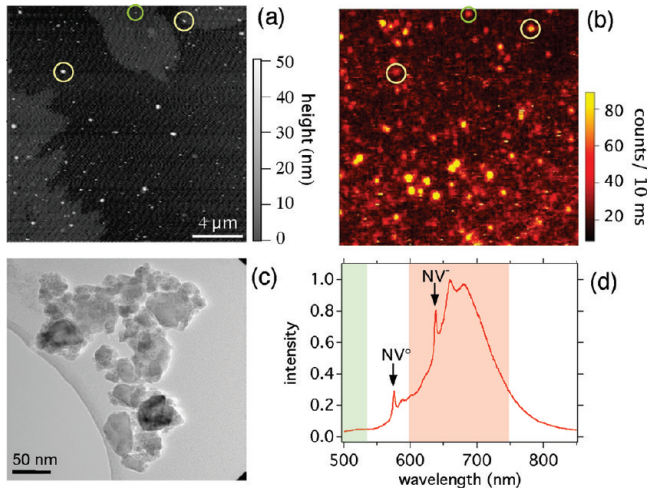


**Figure 5. Simultaneous size and photoluminescence characterization of the PNDs used in this work. The sample is a coverglass on which an aqueous suspension of PNDs is deposited by spin-coating. (a,b) Raster scans (18 × 18 μm) of the same region of the sample in the two modes: (a) AFM and (b) confocal microscopy. For confocal imaging, the excitation laser wavelength is 532 nm, at an excitation power of 200 μW, and the photoluminescence intensity scale bar maximum of graph (b) was set to 90 counts/10 ms in order to be able to observe the less intense PNDs (the brightest spot yields 367 counts/10 ms). Two nanodiamonds of height ~40 nm are circled in yellow, while a 12 nm height nanodiamond is inside the green circle, still displaying a strong photoluminescence signal. (c) High-resolution TEM image of the same type of PNDs. A droplet of the aqueous suspension was initially dried on the carbon grid. (d) Photoluminescence spectrum of NV color centers embedded in the starting micrometer-size diamond crystal (after irradiation and before milling). The narrow lines pointed out by arrows at 575 and 637 nm indicate, respectively, the zero phonon lines of the neutral $NV^0$ and negatively charged $NV^-$ color centers present in this sample. The light red/green rectangles behind NV spectra indicate the spectral range selected by the red/green channels filters, respectively, on the Leica TCS SP2 microscope for PNDs.**

ported in this article deserve to be complemented with correlations between intracellular localization and size, shape, surface chemistry, and incubation time of nanodiamonds with cells.

Finaly, while small PNDs free in the cytosol are ideal candidates for biomolecules transport and/or specific labeling of cellular compartments, big nanoparticles could serve as whole cell labels, due to their high uptake efficiency[26] and their strong photoluminescence or backscattering light signal. Following this strategy, 100 nm in size nanodiamonds were very recently used for labeling and tracking of cell division and differentiation in cancer and stem cells.[41]

## MATERIALS AND METHODS

**Production and Characterization of Photoluminescent Nanodiamonds (PNDs).** The PND production is described in detail in ref 19. Briefly, the starting material was type Ib diamond synthetic micrometer size powder (Element Six, The Netherlands) with a specified size of 150−200 μm. NV centers were created by electron irradiation (irradiation dose $2 \times 10^{18}$ $e^-/cm^2$, beam energy 8 MeV) and subsequent annealing (800 °C, 2 h) in vacuum (pressure $\simeq 10^{-8}$ mbar). Diamond microcrystals were then reduced in size by nitrogen jet milling to obtain submicrometer size crystals (Hosokawa-Alpine, Germany). Further size reduction to nanoparticles was achieved by ball milling under argon (Fritsch, Germany). The milled powder was then sieved and treated by strong sonication (60 min at 50 °C), followed by acid treatment. After rinsing with pure water, filtration, and centrifugation, we obtained PNDs with an average hydrodynamic diameter of 46 nm in a stable water suspension. The size measurement was done by dynamic light scattering (DLS) corrected from Mie scattering, using the DL135 particle size analyzer (Cordouan Technologies, France). The associated zeta potential of this solution was −43 mV (Zetasizer Nano ZS from Malvern, UK).

To simultaneously characterize the PNDs in size and photoluminescence intensity, we used an atomic force microscope (AFM, MFP-3D Asylum Research, USA) coupled to a home-built confocal microscope setup similar to the one depicted on Figure S1 (Supporting Information). For such a study, a droplet of the PND aqueous suspension was deposited by spin-coating on a glass coverslip, which was then simultaneously imaged in AFM (Figure 5a) and photoluminescence (Figure 5b) modes. Among 200 nanodiamonds identified on the AFM scan, 115 display a photoluminescence signal; that is, about 58% of the NDs are photoluminescent. Among the photoluminescent nanoparticles, a small fraction consists of 10−15 nm diameter PNDs, but the majority of the PNDs appear as nano-objects of size 40−50 nm. Some of them form aggregates of 2−3 smaller particles, as can be inferred from TEM imaging (Figure 5c).

**Photoluminescence and Backscattered Light Imaging of Nanodiamonds.** The large-scale photoluminescence observations of PNDs in the cells, which are presented in the main text, are done with a commercial Leica TCS SP2 (Manheim, Germany) laser scanning confocal microscope, with a 63×, 1.4 numerical aperture (NA) oil-immersion objective. Excitation comes from the cw argon ion laser line at 488 nm wavelength. We use one Airy unit as the pinhole diameter for all of the acquisitions. The detection was done in two non-overlapping spectral channels: green channel (500−530 nm) collecting the fluorescence from FITC and LysoTracker−green dye conjugates, and the red channel (600−750 nm) collecting mainly $NV^-$ photoluminescence (see Figure 5d).

For the single-particle analysis presented in the Supporting Information, the photoluminescence was probed using a home-built scanning-stage confocal microscope. It relies on a Nikon TE300 microscope, converted to a confocal setup with the appropriate modifications (refer to Figure S1 of Supporting Information for more details). The microscope objective used is a 60×, 1.4 NA apochromatic oil-immersion objective. The excitation is a cw laser emitting at the wavelength of 488 nm. The photoluminescence signal was acquired by an avalanche photodiode in the single-photon counting mode. This home-built confocal setup is sensitive to the photoluminescence of a single NV color center in a PND, in a cell cultured environment.[21] To record the backscattered excitation laser light, we used a properly oriented quarter-wave plate and polarizing beam splitter cube assembly to redirect all of the reflected light toward another avalanche photodiode in the single-photon counting mode.

For the PND uptake kinetics study, we estimated from the confocal raster scans the mean fluorescence intensity per cell in the red channel. For this purpose, we used the *mean intensity* analysis/measure tool of ImageJ software (NIH, USA). About 40 cells were analyzed for each different incubation time.

**Cell Culture Conditions and Test of Nanodiamond Cytotoxicity.** HeLa cells were grown in standard conditions on glass coverslips in Dulbecco modified Eagle medium (DMEM) supplemented with 10% fetal calf serum (FCS) and 1% penicillin/streptomycin. To study the cellular uptake of PNDs, cells were seeded at a density of $2 \times 10^5$ cells/1.3 $cm^2$ and grown at 37 °C in a humidified incubator under 5% $CO_2$ atmosphere. Twenty-four hours after seeding, the PNDs' aqueous suspension was added to the cell

culture medium. The cells were grown under similar conditions for an additional period of time (from 2 h for fluorescence examination, up to 24 h for the cytotoxicity tests). After incubation, the excess of PNDs was removed by washing the cells with phosphate buffer saline (PBS). The cells were then fixed with 4% paraformaldehyde in PBS and mounted on microscope slides for phase contrast and confocal microscopy studies.

**Cellular Uptake of Nanodiamonds.** To investigate the uptake mechanism of PNDs, cells were treated as follows:

***Experiments Blocking the Endocytosis (Energy-Dependent Process):*** For low-temperature incubation, cells were grown as described above with the cell culture kept at 4 °C instead of 37 °C. For the incubation with PNDs under ATP depletion, the cells were preincubated in PBS buffer, supplemented with 10 mM $NaN_3$ during 30 min at 37 °C, and then PNDs were added.

For the investigation of the type of receptor-mediated endocytosis mechanism, cells were treated as follows:

***Hypertonic Treatment to Hinder the Clathrin-Mediated Process:*** The cells were preincubated for 30 min in PBS buffer supplemented with 0.45 M sucrose followed by incubation with PNDs at 37 °C.

***Filipin Treatment Blocking Caveolae Pathway:*** The cells were pretreated in PBS buffer and supplemented with filipin (5 μg/mL) for 30 min before exposure to PNDs at 37 °C.

For PNDs intracellular localization analyses by immunofluorescence, the endosomes were labeled with FITC-conjugated mouse antihuman early endosome antigen EEA1 (ref. 612006, BD Transduction Laboratories, USA).[21] FITC dye has absorption/emission maxima at 490/520 nm, respectively. The lysosomes were labeled with LysoTracker Green DND-26 dye (L7526, Invitrogen, USA), with absorption/emission maxima at 504/511 nm, respectively. After 2 h of incubation of PNDs at 37 °C with the cells, the medium was replaced with prewarmed new medium containing the LysoTracker probe (75 nM) for one additional hour of incubation. The medium was then replaced with fresh medium just before cell fixation as described above.

**Transmission Electron Microscopy.** The electron microscopy observations were done with a high-resolution transmission electron microscope (HR-TEM, Tecnai F20 operating at 200 keV). Cells were seeded for 24 h in standard conditions (conditions similar to those used for fluorescence experiments). PNDs were added in cell culture medium and incubated for 2 h at 37 °C. Cells were then fixed in a solution of paraformaldehyde, glutaraldehyde, and phosphate buffer for 45 min at room temperature. After dehydration with a graded series of ethanol, the cells were embedded in EPON resin. Ultrathin sections of the resin block were then cut (100 nm thickness) and stained with 2% uranyl acetate for a higher contrast imaging under the HR-TEM microscope.

*Acknowledgment.* We are grateful to Jean-François Roch and Karen Perronet for fruitful discussions. We thank Géraldine Dantelle for the measurements of diamond colloidal suspensions and zeta potentials, Abdallah Slablab for the confocal scan measurement coupled with the AFM setup, and Anne Tarrade for the preparation of the samples observed with transmission electron microscopy. This work was supported by the European Commission through the project "Nano4Drugs" (Contract LSHB-2005-CT-019102), by Agence Nationale de la Recherche through the project "NaDia" (Contract ANR-2007-PNANO-045), and by the "Ile-de-France Region" through the grant C'Nano IdF "BioDiam", and the grant "Aide au portage du projet Nano4drugs".

*Supporting Information Available:* The home-built scanning confocal microscopy setup is described on Figure S1. This microscope has a single NV color center sensitivity, allowing the observation of the smallest PNDs. It was used for a more precise comparison of the photoluminescence and the backscattered signal coming from PNDs deposited on a glass-coverslip (Figure S2). It was also used for PNDs observation in cultured cell, in particular, to show that even the smallest PNDs are not internalized when they are incubated at 4 °C with HeLa cells (Figure S5); and finally to make a high sensitivity colocalization study of PNDs with endosomes (Figure S7). Additional observations done with the commercial Leica TCS SP2 are shown in Figure S3 (graph representing the dynamics of photoluminescent nanodiamonds uptake by HeLa cells) and Figure S4 (3D reconstruction of confocal raster scans showing the localization of PNDs in the cell of Figure 1). For the colocalization studies, we checked that there is no crosstalk between PNDs and FITC detection channels (Figure S6). We also provide additional high-resolution TEM images of a HeLa cell incubated with PNDs (Figure S8). The surface function characterization by Fourier transform infrared (FT-IR) spectroscopy of nanodiamonds before and after mixture with the fetal calf serum is explained in detail with the spectra provided on Figure S9. The cytotoxicity test results of PNDs incubated with HeLa cells are presented on Figure S10. This material is available free of charge *via* the Internet at http://pubs.acs.org.

## REFERENCES AND NOTES

1. Alivisatos, P. The Use of Nanocrystals in Biological Detection. *Nat. Biotechnol.* **2004**, *22*, 47–52.
2. Michalet, X.; Pinaud, F.; Bentolila, L.; Tsay, J.; Doose, S.; Li, J.; Sundaresan, G.; Wu, A.; Gambhir, S.; Weiss, S. Quantum Dots for Live Cells, *In Vivo* Imaging, and Diagnostics. *Science* **2005**, *307*, 538–544.
3. Lasne, D.; Blab, G.; Berciaud, S.; Heine, M.; Groc, L.; Choquet, D.; Cognet, L.; Lounis, B. Single Nanoparticle Photothermal Tracking (SNaPT) of 5-nm Gold Beads in Live Cells. *Biophys. J.* **2006**, *91*, 4598–4604.
4. Warner, J.; Hoshino, A.; Yamamoto, K.; Tilley, R. Water-Soluble Photoluminescent Silicon Quantum Dots. *Angew. Chem., Int. Ed.* **2005**, *44*, 4550–4554.
5. Resch-Genger, U.; Grabolle, M.; Cavaliere-Jaricot, S.; Nitschke, R.; Nann, T. Quantum Dots *versus* Organic Dyes as Fluorescent Labels. *Nat. Methods* **2008**, *9*, 763–775.
6. Kirchner, C.; Liedl, T.; Kudera, S.; Pellegrino, T.; Javier, A.; Gaub, H.; Stoelze, S.; Fertig, N.; Parak, W. Cytotoxicity of Colloidal CdSe and CdSe/ZnS Nanoparticles. *Nano Lett.* **2005**, *5*, 331–338.
7. Nirmal, M.; Dabbousi, B.; Bawendi, M.; Macklin, J.; Trautman, J.; Harris, T.; Brus, L. Fluorescence Intermittency in Single Cadmium Selenide Nanocrystal. *Nature* **1996**, *383*, 802–804.
8. Gruber, A.; Dräbenstedt, A.; Tietz, C.; Fleury, L.; Wrachtrup, J.; Von Borczyskowsky, C. Scanning Confocal Optical Microscopy and Magnetic Resonance on Single Defect Centers. *Science* **1997**, *276*, 2012–2014.
9. Faklaris, O.; Garrot, D.; Joshi, V.; Boudou, J.-P.; Sauvage, T.; Curmi, P. A.; Treussart, F. Comparison of the Photoluminescence Properties of Semiconductor Quantum Dots and Non- Blinking Diamond Nanoparticles and Observation of the Diffusion of Diamond Nanoparticles in Living Cells. *J. Eur. Opt. Soc. Rap. Public* **2009**, *4*, 09035.
10. Neugart, F.; Zappe, A.; Jelezko, F.; Tietz, C.; Boudou, J.-P.; Krueger, A.; Wrachtrup, J. Dynamics of Diamond Nanoparticles in Solution and Cells. *Nano Lett.* **2007**, *7*, 3588–3591.
11. Chang, Y.-R.; Lee, H.-Y.; Chen, K.; Chang, C.-C.; Tsai, D.-S.; Fu, C.-C.; Lim, T.-S.; Tzeng, Y.-K.; Fang, C.-Y.; Han, C.-C.; *et al.* Mass Production and Dynamic Imaging of Fluorescent Nanodiamonds. *Nat. Nanotechnol.* **2008**, *3*, 284–288.
12. Krüger, A. Diamond Nanoparticles for Biological Applications. *Chem.—Eur. J.* **2008**, *14*, 1382–1390.
13. Liang, Y.; Ozawa, M.; Krüger, A. A General Procedure to Functionalize Agglomerating Nanoparticles Demonstrated on Nanodiamond. *ACS Nano* **2009**, *3*, 2288–2296.
14. Chao, J.-I.; Perevedentseva, E.; Chung, P.-H.; Liu, K.-K.; Cheng, C.-Y.; Chang, C.-C.; Cheng, C.-L. Nanometer-Sized Diamond Particle as a Probe for Biolabeling. *Biophys. J.* **2007**, *93*, 2199–2208.
15. Vial, S.; Mansuy, C.; Sagan, S.; Irinopoulou, T.; Burlina, F.; Boudou, J.-P.; Chassaing, G.; Lavielle, S. Peptide-Grafted Nanodiamonds: Preparation, Cytotoxicity and Uptake in Cells. *ChemBioChem* **2008**, *9*, 2113–2119.
16. Mkandawire, M.; Pohl, A.; Gubarevich, T.; Lapina, V.; Appelhans, D.; Rödel, G.; Pompe, W.; Schreiber, J.; Opitz, J. Selective Targeting of Green Fluorescent Nanodiamond Conjugates to Mitochondria in HeLa Cells. *J. Biophotonics* **2009**, 296–606.

17. Huang, H.; Pierstorff, E.; Osawa, E.; Ho, D. Active Nanodiamond Hydrogels for Chemotherapeutic Delivery. *Nano Lett.* **2007**, *7*, 3305–3314.
18. Chen, M.; Pierstorff, E.; Lam, R.; Li, S.-Y.; Huang, H.; Osawa, E.; Ho, D. Nanodiamond- Mediated Delivery of Water-Insoluble Therapeutics. *ACS Nano* **2009**, *3*, 2016–2022.
19. Boudou, J.-P.; Curmi, P. A.; Jelezko, F.; Wrachtrup, J.; Aubert, P.; Sennour, M.; Balasubramanian, G.; Reuter, R.; Thorel, A.; Gaffet, E. High Yield Fabrication of Fluorescent Nanodiamonds. *Nanotechnology* **2009**, *20*, 235602.
20. Fu, C.-C.; Lee, H.-Y.; Chen, K.; Lim, T.-S.; Wu, H.-Y.; Lin, P.-K.; Wei, P.-K.; Tsao, P.-H.; Chang, H.-C.; Fann, W. Characterization and Applications of Single Fluorescent Nanodiamonds as Cellular Biomarkers. *Proc. Natl. Acad. Sci. U.S.A.* **2007**, *104*, 727.
21. Faklaris, O.; Garrot, D.; Joshi, V.; Druon, F.; Boudou, J.-P.; Sauvage, T.; Georges, P.; Curmi, P. A.; Treussart, F. Detection of Single Photoluminescent Diamond Nanoparticles in Cells and Study of Their Internalization Pathway. *Small* **2008**, *4*, 2236–2239.
22. Schrand, A. M.; Huang, H.; Carlson, C.; Schlager, J.; Osawa, E.; Hussain, S.; Dai, L. Are Diamond Nanoparticles Cytotoxic? *J. Phys. Chem. B* **2007**, *111*, 2–7.
23. Smith, B.-R.; Niebert, M.; Plakhotnik, T.; Zvyagin, A.-V. Transfection and Imaging of Diamond Nanocrystals as Scattering Optical Labels. *J. Lumin.* **2007**, *127*, 260.
24. Colpin, Y.; Swan, A.; Zvyagin, A.; Plakhotnik, T. Imaging and Sizing of Diamond Nanoparticles. *Opt. Lett.* **2006**, *31*, 625.
25. Wee, T.-L.; Mau, Y.-W.; Fang, C.-Y.; Hsu, H.-L.; Han, C.-C.; Chang, H.-C. Preparation and Characterization of Green Fluorescent Nanodiamonds for Biological Applications. *Diamond Relat. Mater.* **2009**, *18*, 567–573.
26. Chithrani, B.; Ghazani, A.; Chan, W.-C. Determining the Size and Shape Dependence of Gold Nanoparticle Uptake into Mammalian Cells. *Nano Lett.* **2006**, *6*, 662–668.
27. Marsh, M.; McMahon, H. Cell Biology—The Structural Era of Endocytosis. *Science* **1999**, *285*, 215.
28. Murkherjee, S.; Ghosh, R.; Maxfield, F. Endocytosis. *Physiol. Rev.* **1997**, *77*, 759–803.
29. Schmid, S.; Carter, L. ATP is Required for Receptor-Mediated Endocytosis in Intact Cells. *J. Cell Biol.* **1990**, *111*, 2307–2318.
30. Steinman, R.; Mellman, I.; Muller, W.; Cohn, Z. Endocytosis and the Recycling of Plasma Membrane. *J. Cell Biol.* **1983**, *96*, 1–27.
31. Mousavi, S.; Malerod, L.; Berg, T.; Kjeken, R. Clathrin-Dependent Endocytosis. *Biochem. J.* **2004**, *377*, 1–16.
32. Pelkmans, L.; Brli, T.; Zerial, M.; Helenius, A. Caveolin-Stabilized Membrane Domains as Multifunctional Transport and Sorting Devices in Endocytic Membrane Traffic. *Cell* **2004**, *118*, 767–780.
33. Heuser, J.; Anderson, R. Hypertonic Media Inhibit Receptor-Mediated Endocytosis by Blocking Clathrin-Coated Pit Formation. *J. Cell Biol.* **1989**, *108*, 389–400.
34. Qaddoumi, M.; Gukasyan, H.; Davda, J.; Labhasetwar, V.; Kim, K.; Lee, V. Clathrin and Caveolin-1 Expression in Primary Pigmented Rabbit Conjunctival Epithelial Cells: Role in PLGA Nanoparticle Endocytosis. *Molec. Vis.* **2003**, *9*, 559–568.
35. Kruth, H.; Vaughan, M. Quantification of Low Density Lipoprotein Binding and Cholesterol Accumulation by Single Human Fibroblasts Using Fluorescence Microscopy. *J. Lipid Res.* **1980**, *21*, 123–130.
36. Kam, N.; Liu, Z.; Dai, H. Carbon Nanotubes as Intracellular Transporters for Proteins and DNA: An Investigation of the Uptake Mechanism and Pathway. *Angew. Chem., Int. Ed.* **2006**, *45*, 577–581.
37. Treussart, F.; Jacques, V.; Wu, E.; Gacoin, T.; Grangier, P.; Roch, J.-F. Photoluminescence of Single Colour Defects in 50 nm Diamond Nanocrystals. *Physica B* **2006**, *376*, 926–929.
38. Jaiswai, J.-K.; Mattoussi, H.; Mauro, J.; Simon, S.-M. Long-Term Multiple Color Imaging of Live Cells Usings Quantum Dot Bioconjugates. *Nat. Biotechnol.* **2002**, *21*, 47.
39. Nativo, P.; Prior, I.; Brust, M. Uptake and Intracellular Fate of Surface-Modied Gold Nanoparticles. *ACS Nano* **2008**, *2*, 1639–1644.
40. We checked by carrying out a local area Fourier transform electron diffractogram on one of the TEM dark spots of size ≃10 nm that it has the signature of diamond material (inset of Figure 4e).
41. Liu, K.-K.; Wang, C.-C.; Cheng, C. L.; Chao, J.-I. Endocytic Carboxylated Nanodiamond for the Labeling and Tracking of Cell Division and Differentiation in Cancer and Stem Cells. *Biomaterials* **2009**, *30*, 4249–4259.
42. Lewinski, N.; Colvin, V.; Drezek, R. Cytotoxicity of Nanoparticles. *Small* **2008**, *4*, 26–49.